Partitioning of CO_2 sources in Nanjing using $\delta^{13}C$ tracer

Reporter: Jiaping Xu

2014-8-22

Outline

- 1. Background
- 2. Objective
- 3. Material and Method
- 4. Preliminary results
- 5. Conclusions
- 6. Next work

1. Background

- The CO_2 emission contributed by fossil fuel combustion in Yangtze River Delta (YRD) can break original carbon balance in this area.

- Monitoring CO_2 concentration and its ^{13}C isotopic composition by high frequency instrument and energy-use statistics method, we can calculate CO_2 flux density and partition the CO_2 contributors. This can greatly help us to understand the different roles played by natural and anthropogenic CO_2 sources in urban areas.

$\delta^{13}C$ can be used as a good carbon tracer.

Keeling Plot (D. E. Pataki, et al., 2003)

$$C_a = C_b + C_s \quad \text{(Eq.1)}$$

$$C_a\delta_a = C_b\delta_b + C_s\delta_s \quad \text{(Eq.2)}$$

$$\delta^{13}C_a = C_b(\delta^{13}C_b - \delta^{13}C_s)(1/C_a) + \boxed{\delta^{13}C_s} \quad \text{(Eq.3)}$$

Miller-Tans Method (Miller, P P. Tans, 2003)

$$\delta_a C_a - \delta_b C_b = \boxed{\delta^{13}C_s}(C_a - C_b) \quad \text{(Eq.4)}$$

slowly varying
3-month moving box car
(Data from MLO site, 2012)

- C: Concentration
- δ: Isotopic ratio
- a: Atmosphere
- b: Background
- s: Mixing sources

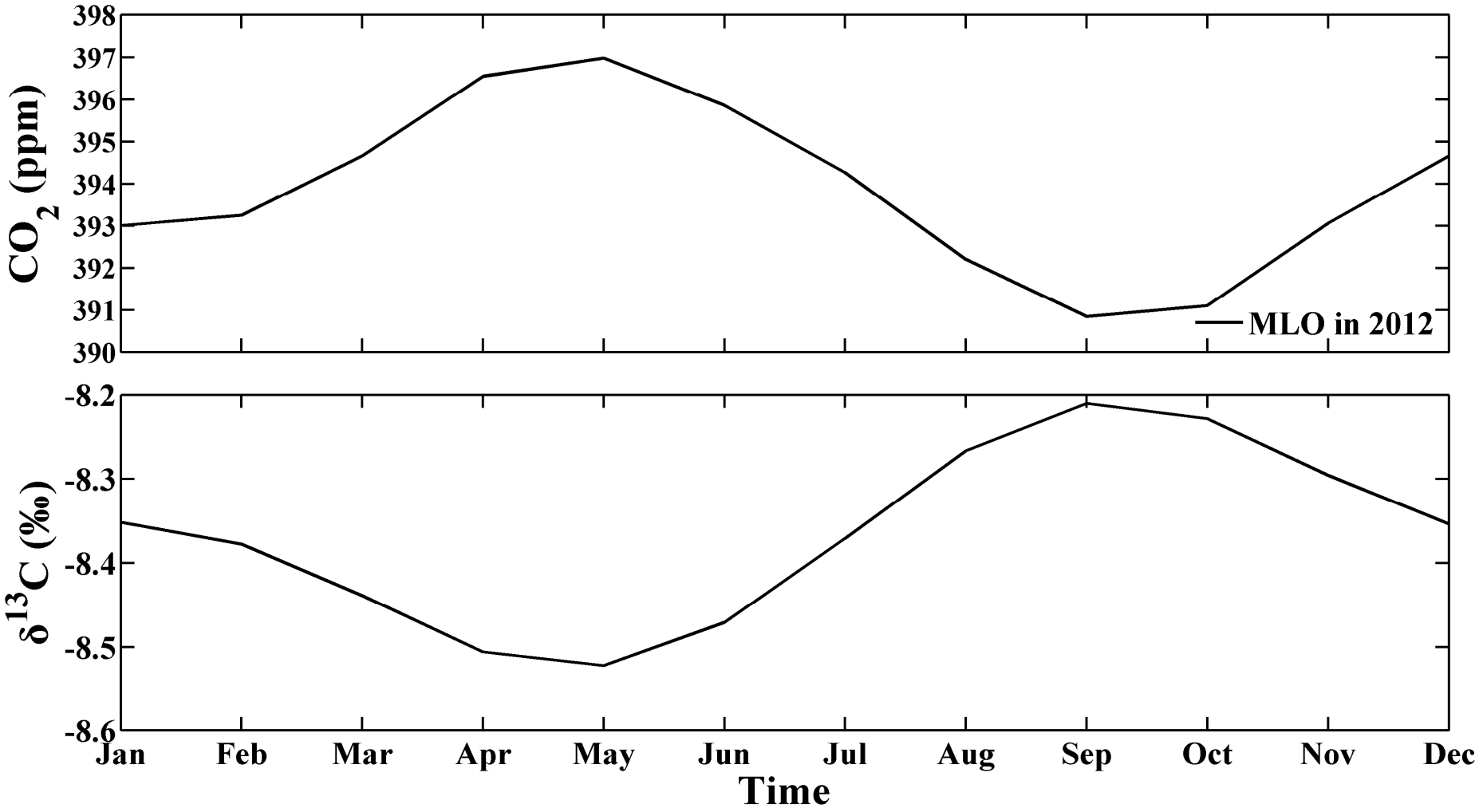

Fig. 1. Monthly CO_2 and $\delta^{13}C$ at MLO in 2012.

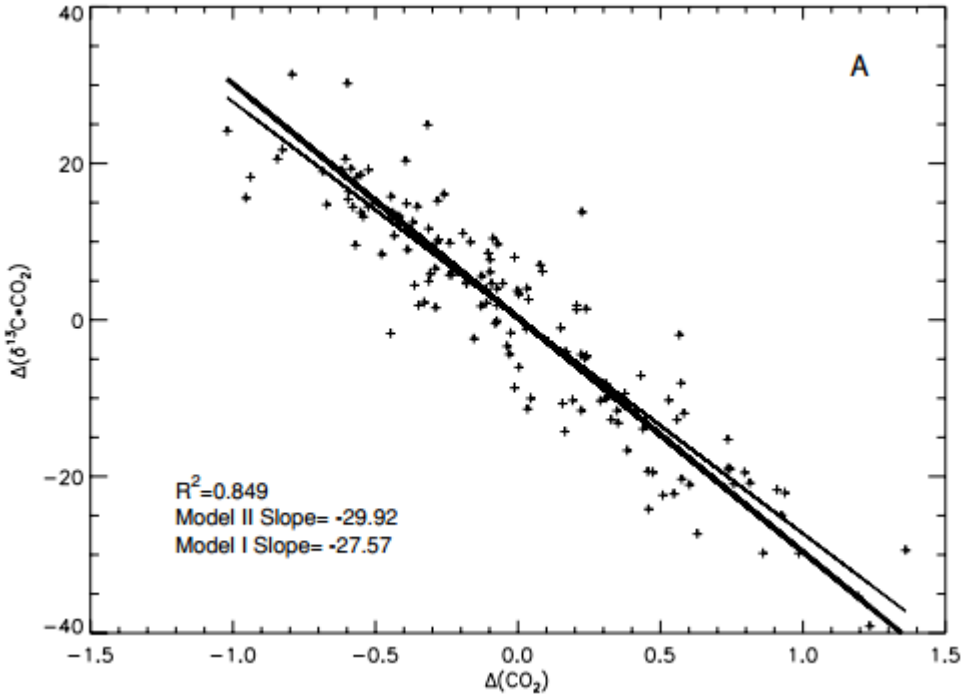

Fig.2. Miller-Tans method

(Miller, P P. Tans, 2003)

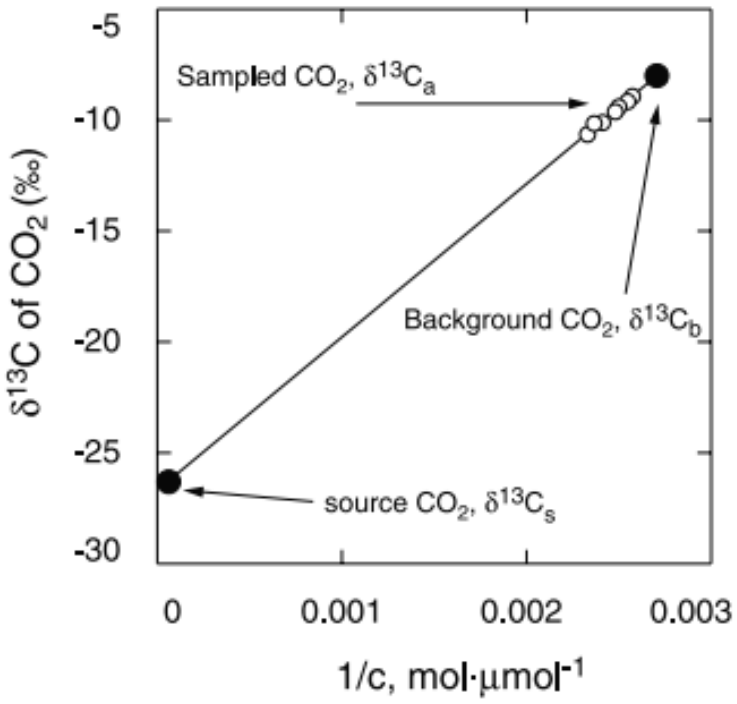

Fig.3. Keeling plot

(D. E. Pataki, et al., 2003)

The approach of monthly CO_2 flux calculation

$$F_N = F_F + F_C + F_P \quad \text{(Eq.5)}$$

$$\delta_N F_N = \delta_F F_F + \delta_C F_C + \delta_P F_P \quad \text{(Eq.6)}$$

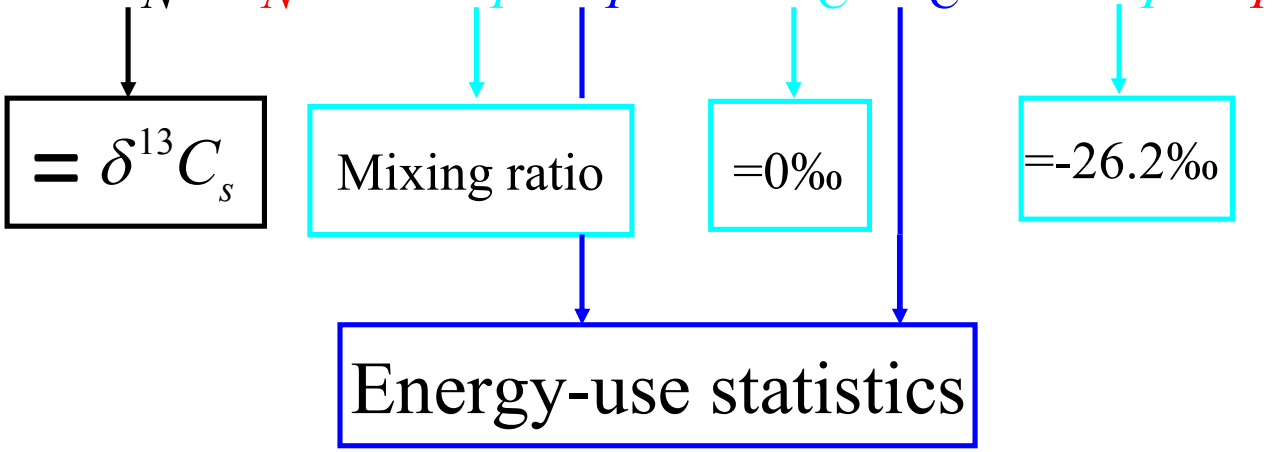

F_N: Net CO_2 flux density (CO_2mg·m^{-2}·s^{-1})
F_F: Fossil fuel combustion CO_2 flux density
F_C: Clink production CO_2 flux density
F_P: Plant CO_2 flux density
δ : Isotope ratio

2. Objective

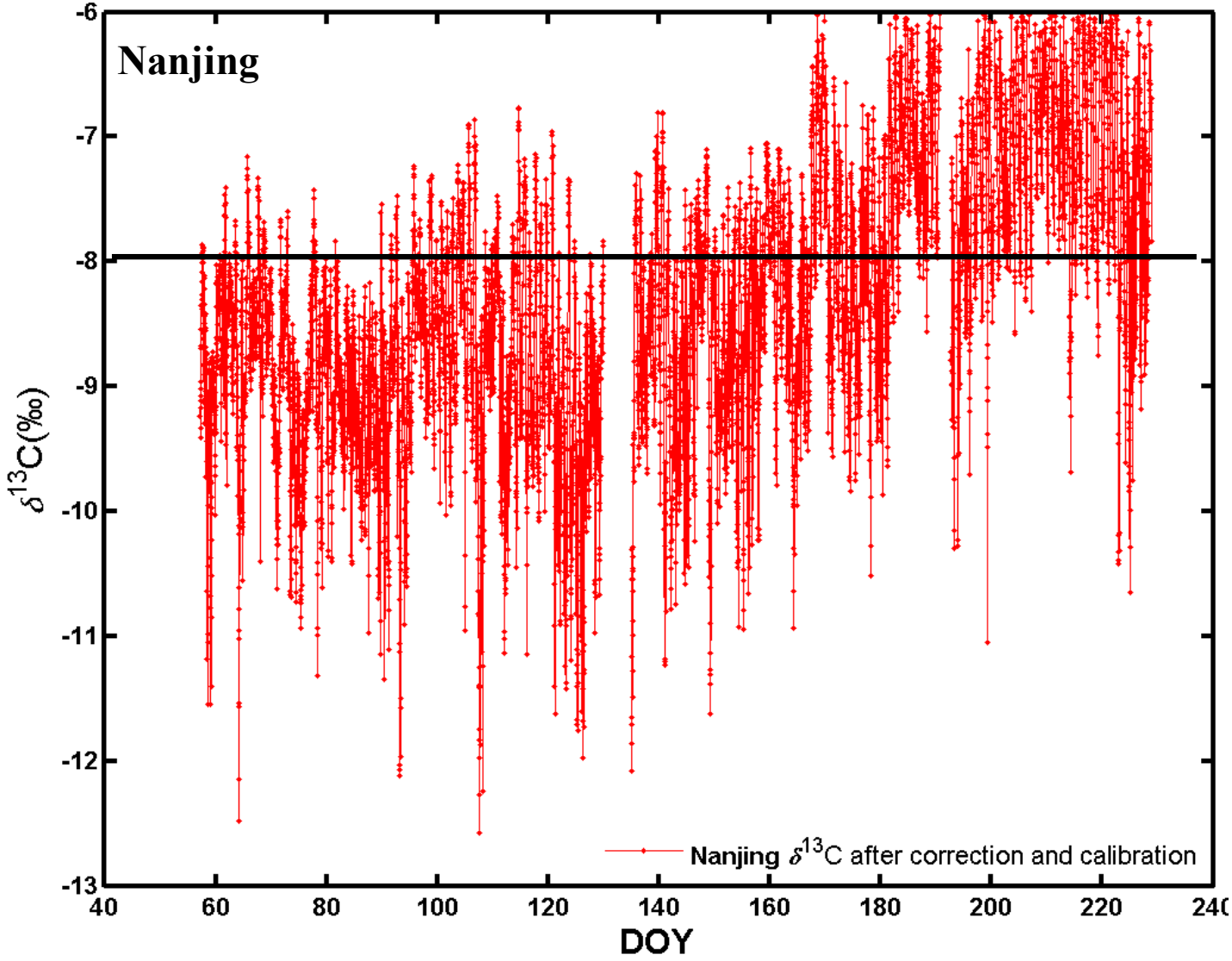

Fig. 4.The time series of δ^{13}C in Nanjing in 2013.

- 1. Calculate monthly $\delta^{13}C_S$ in Nanjing by Keeling and Miller-Tans method.
- 2. Calculate CO_2 fossil fuel combustion estimated with the IPCC inventory method and its mixing $\delta^{13}C$.
- 3. Produce a clink/cement CO_2 flux density map of Eastern China.
- 4. Determine the source region by using back trajectory analysis and WPSCF.
- 5. Partition the total CO_2 emission source into fossil fuel combustion, cement production and plant respiration.
- 6. Analyze the sensitivity and uncertainty of mean contributions by each fractional CO_2 flux in YRD.

3. Material and Method

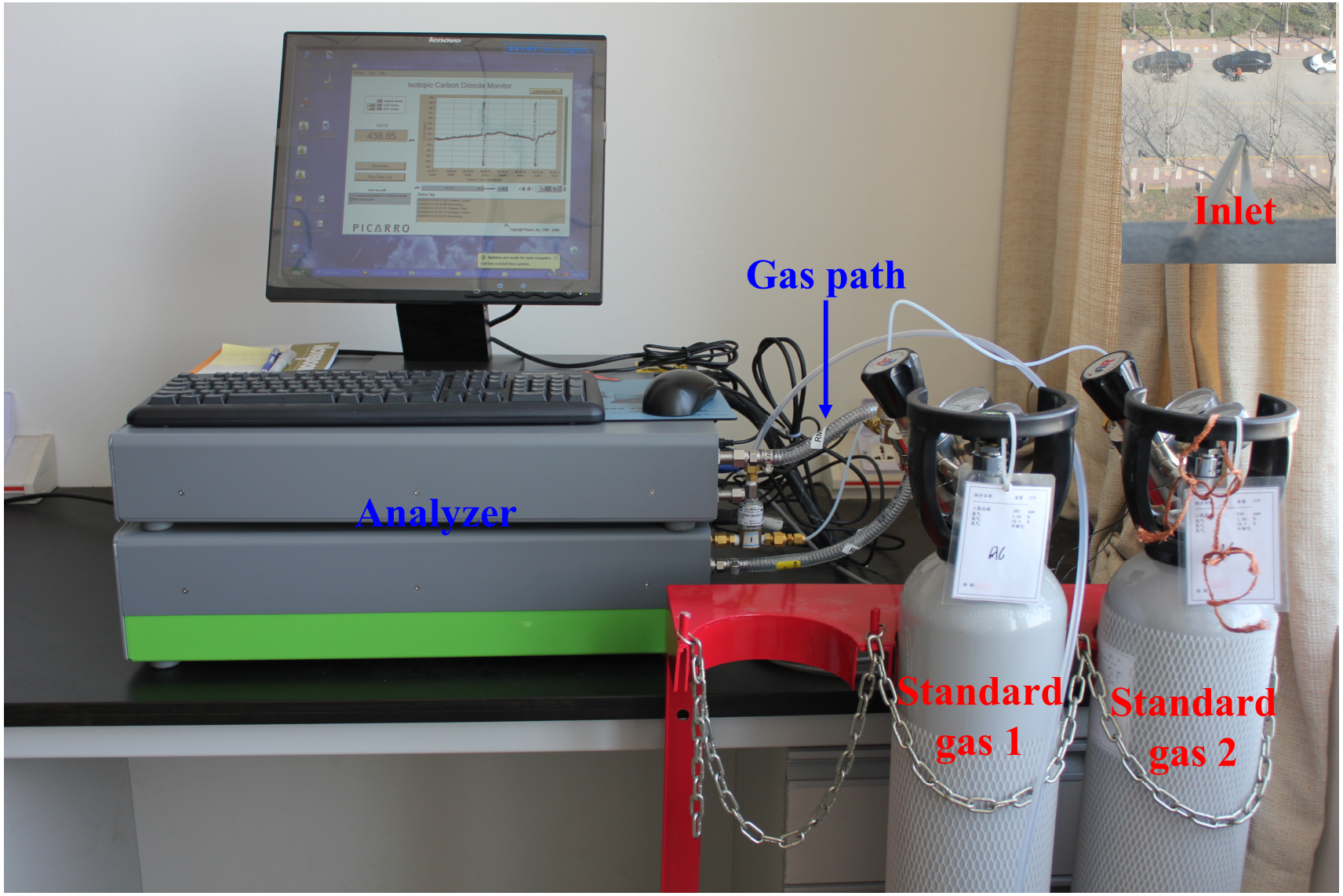

Fig. 5. CO_2 and its stable isotopic composition analyzer (Picarro G1101-i) and calibration system in Nanjing.

Table 2. Dataset of Picarro.

Sites	Period of time
NUIST	26th Feb, 2013~9th August, 2014

Table 3. Cycling of measurement.

Gases	Lasting Time (min)
Standard gas 1	5
Standard gas 2	5
Ambient air	170

Table 4. Information of standard gases.

Gases	CO_2 concentration (ppm)	$\delta^{13}C$*(‰)
Standard gas 1	380	-29.75 ± 0.27
Standard gas 2	500	-30.01 ± 0.18

* (n=41) Results from CAAS and CAFS.

Data processing

- 1. Remove methane data
- 2. Remove 3 minutes data after switchover (about 44 data)
- 3. Filter outliers
- 4. Calibrate raw data by 2-point standard gases calibration
- 5. Average data into 1 hour
- 6. Calculate $\delta^{13}C_S$ by Miller's method.

4. Preliminary results

4.1. $\delta\,^{13}C_S$ calculated by Bowling and Miller-Tans method

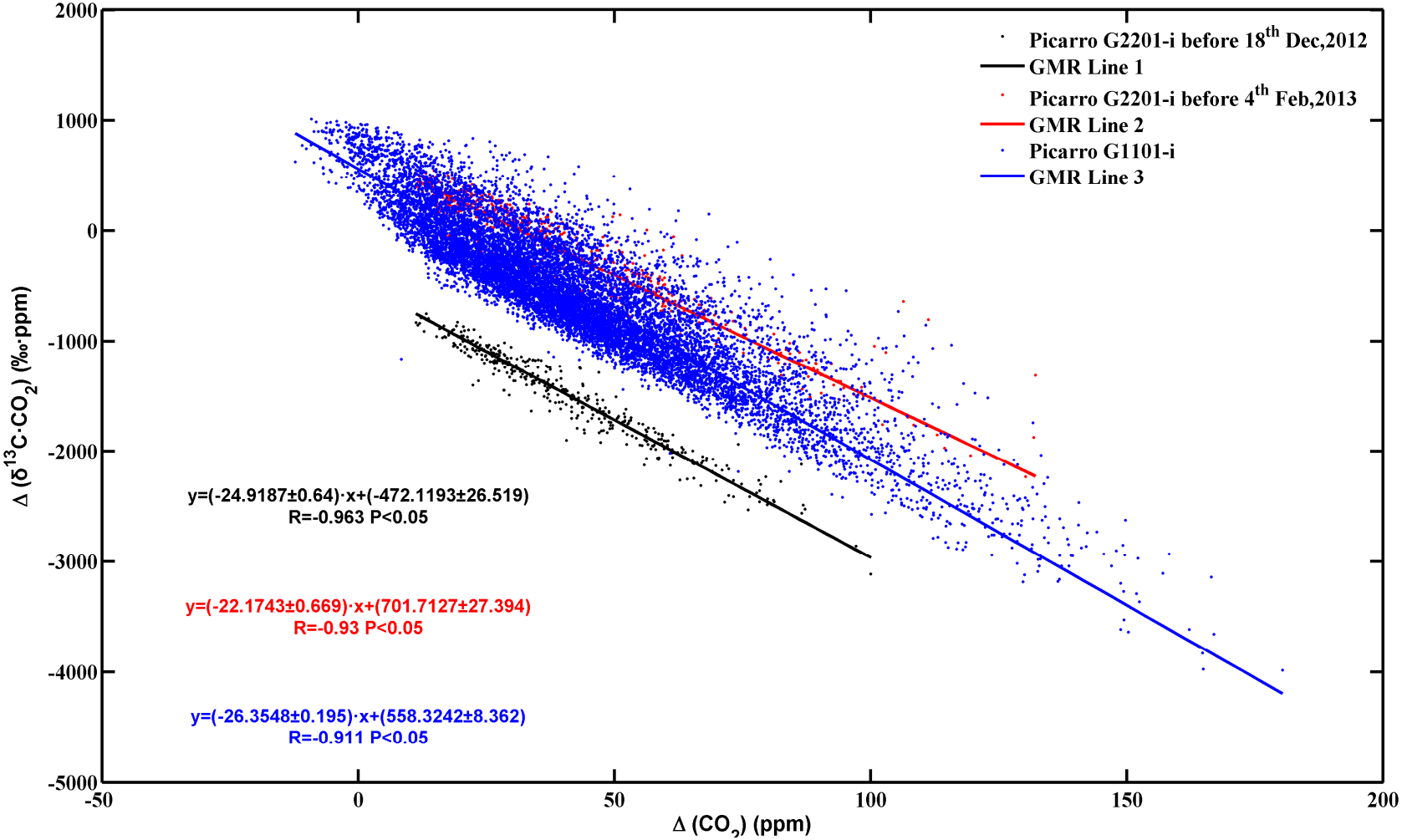

Fig. 6. Keeling $\delta^{13}C_s$ in Nanjing from 26th Feb, 2013 to 20th August, 2014.

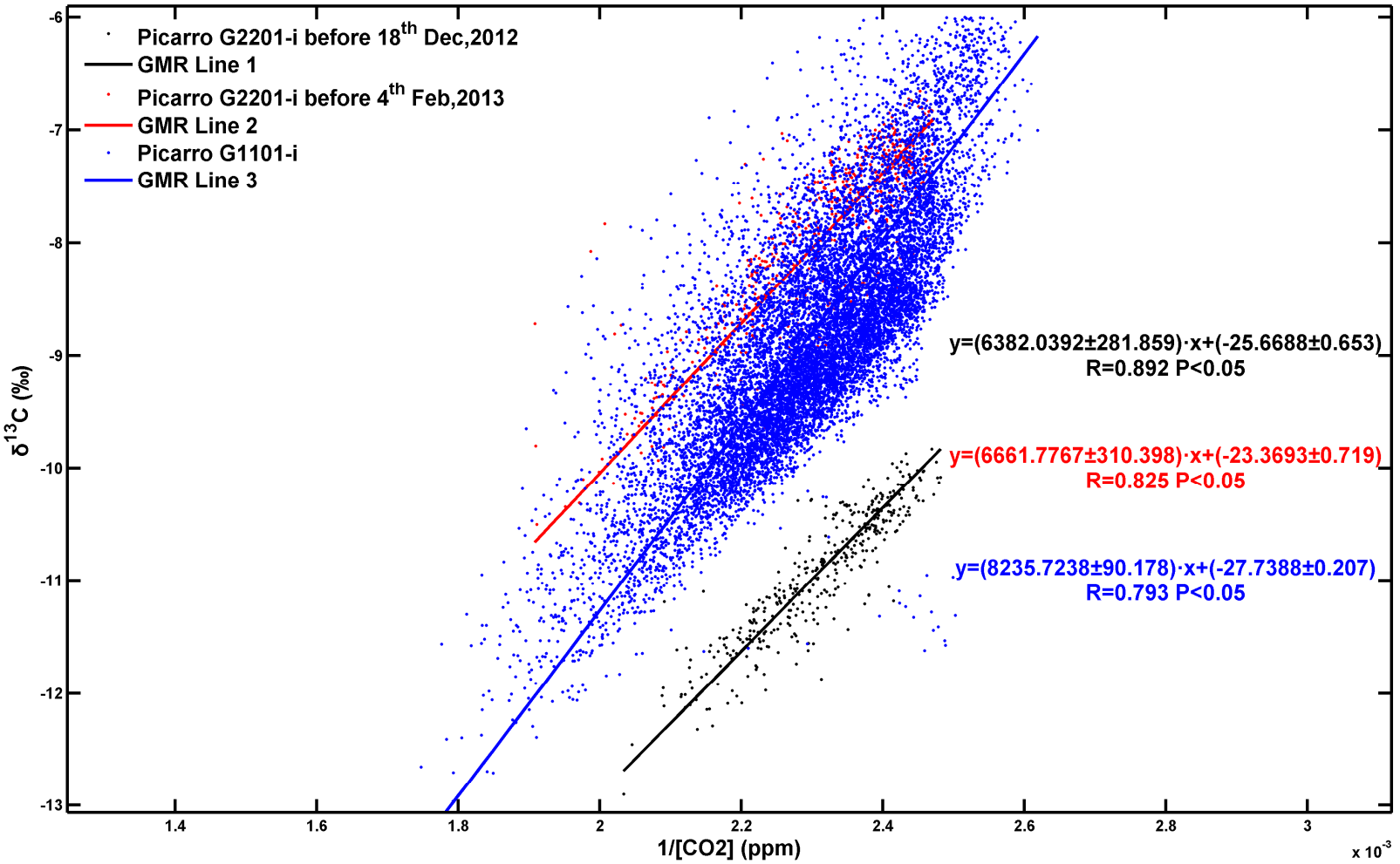

Fig. 7. Miller-Tans $\delta^{13}C_s$ in Nanjing from 26th Feb, 2013 to 20th August, 2014.

Table 5. Monthly variation of $\delta^{13}C_s$.

Months	Miller		Keeling	
	$\delta^{13}C_s$(‰)	R	$\delta^{13}C_s$(‰)	R
Feb,2013	-25.566 ±0.77	-0.985	-25.878 ± 0.783	0.961
Mar,2013	-24.451 ±0.499	-0.958	-25.104 ± 0.524	0.892
Apr,2013	-25.441 ±0.505	-0.963	-26.066 ± 0.538	0.904
May,2013	-25.183 ±0.492	-0.969	-25.6905 ± 0.506	0.923
Jun,2013	-25.572 ±0.659	-0.935	-26.544 ± 0.682	0.851
Jul,2013	-24.150 ±0.614	-0.942	-24.910 ± 0.638	0.882
Aug,2013	-24.667 ±1.001	-0.877	-26.396 ± 1.032	0.761
Sep,2013	-22.176±0.563	-0.938	-22.927 ± 0.899	0.828
Oct,2013	-24.029±0.423	-0.972	-24.649 ± 0.444	0.925
Nov,2013	-23.028±0.66	-0.952	-23.923 ± 1.238	0.878
Dec,2013	-23.514±0.326	-0.981	-25.9234 ± 0.331	0.948
Jan,2014	-24.355±0.464	-0.971	-24.888 ± 0.42	0.924
Feb,2014	-23.432±0.605	-0.964	-24.093± 0.478	0.905
Mar,2014	-23.8705±0.44	-0.967	-24.463 ± 0.465	0.929
Apr,2014	-24.242±0.41	-0.972	-24.756± 0.426	0.868
May,2014	-25.324±0.587	-0.945	-25.132 ± 0.593	0.887
Jun,2014	-22.79±0.489	-0.955	-23.498± 0.501	0.783
Jul,2014	-21.626±0.656	-0.907	-22.944± 0.679	0.804

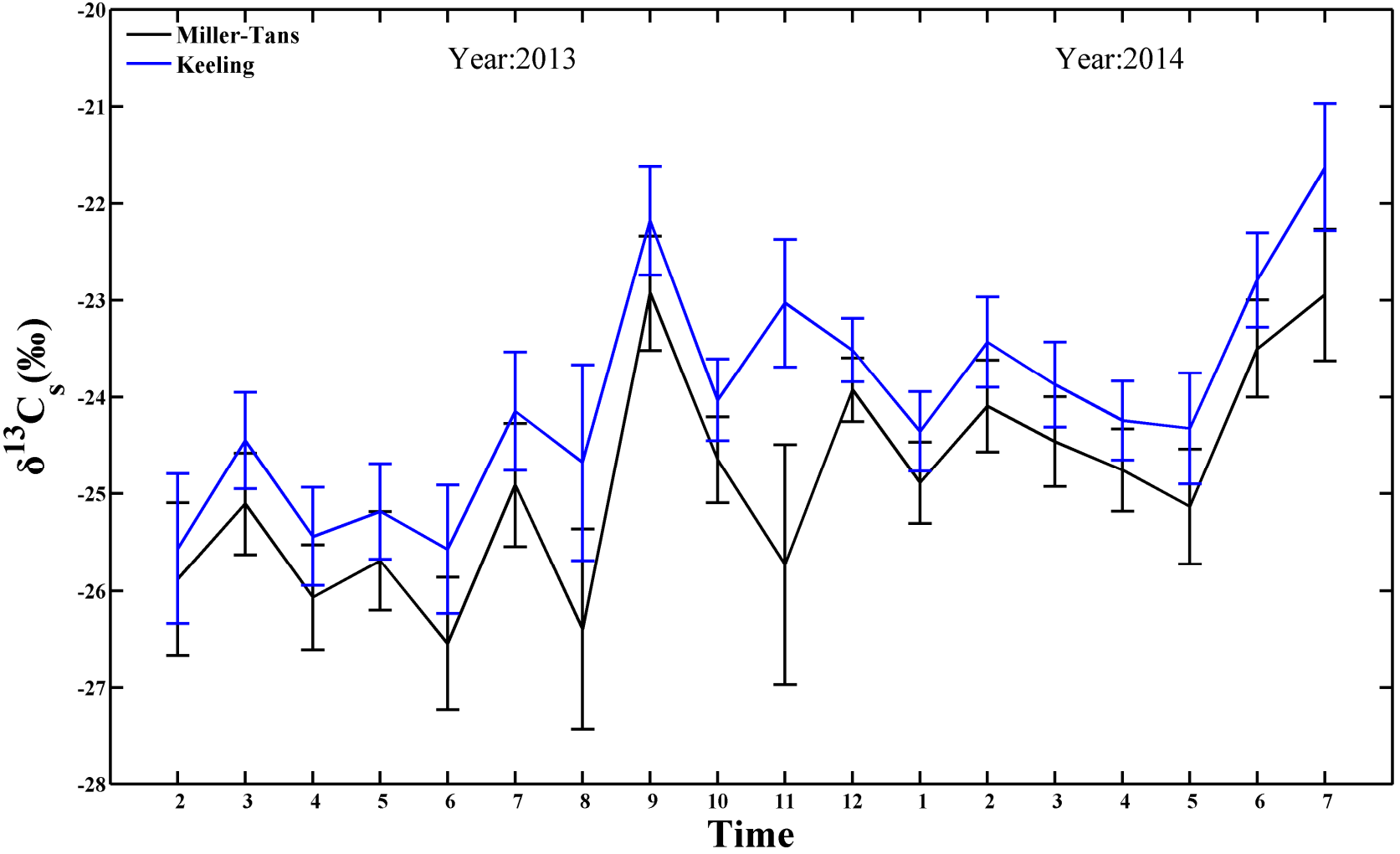

Fig. 7. The time series of $\delta^{13}C_s$ based on Miller-Tans and Keeling method in Nanjing.

4.2. CO_2 fossil fuel combustion and its $\delta^{13}C_S$

Table.6. CO_2 emission factors in IPCC.

Carbon Sources	Emission factors
Coal	1.98
Coke	3.02
Crude Oil	3.1
Gasoline	3.18
Kerosene	3.15
Diesel	3.18
Furnace	3.13
Natural Gas	21.84
Clink	0.52

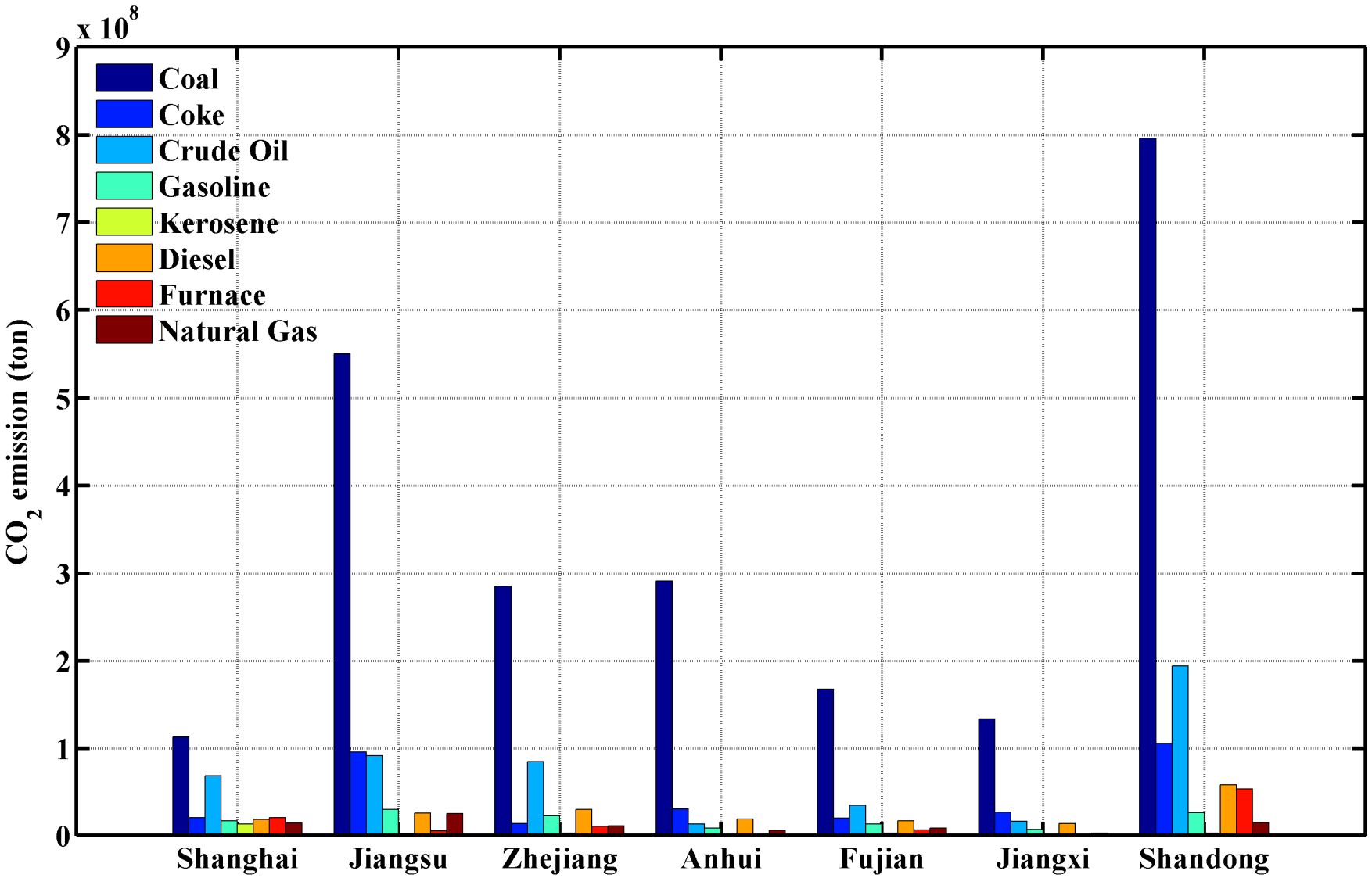

Fig. 8. Fossil CO2 emission in Nanjing in 2012.

F_F inYRD:0.1744 (CO_2 mg·m^{-2}·s^{-1}), in this study.
0.2357(CO_2 mg·m^{-2}·s^{-1}), Carbon tracer.

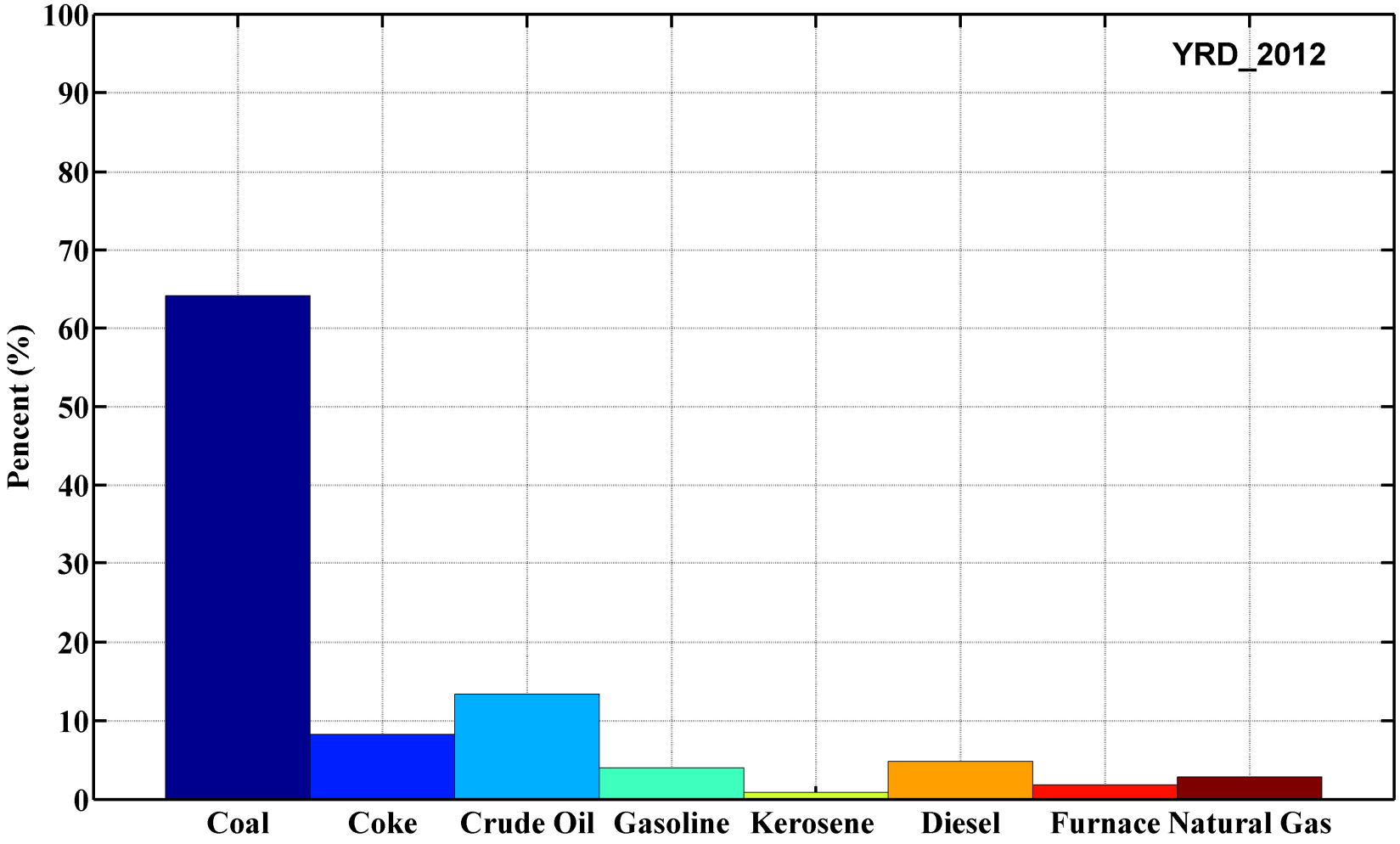

Fig. 9. The fractional contribution of fossil combustion in Nanjing in 2012.

Table.7. $\delta^{13}C$ in Fossil.

Carbon Sources	$\delta^{13}C$ (‰)	Reference
Coal	-23.97	Xu YC,1990
Coke	-24	Xu YC,1990
Crude Oil	-28.16	Xu YC,1990
Gasoline	-28.4	S.E. Bush,2007
Kerosene	-29.3	Andes,2000
Diesel	-28.3	S.E. Bush,2007
Furnace	-37.1	S.E. Bush,2007
Natural Gas	-37.7	Pataki,2003
Total	-25.59	This study

4.3. Cement/Clink CO_2 flux density map

Table.8 The number of sizeable production plants in Eastern China.

Province	Number
Jiangsu	33
Zhejiang	29
Anhui	40
Fujian	60
Jiangxi	33
Shandong	30
Shanghai	0

Table.9 The number of production lines in Eastern China.

	Production (1000ton/day)							
Province	<1	1-2	2-3	3-4	4-5	5-10	>10	
Jiangsu	0	6	16	3	2	29	2	1
Zhejiang	0	15	35	0	1	21	0	4
Anhui	0	4	22	0	4	53	6	
Fujian	0	2	24	1	4	18	0	
Jiangxi	0	7	23	2	5	20	0	
Shandong	0	6	32	0	17	33	0	
Shanghai	0	0	0	0	0	0	0	0

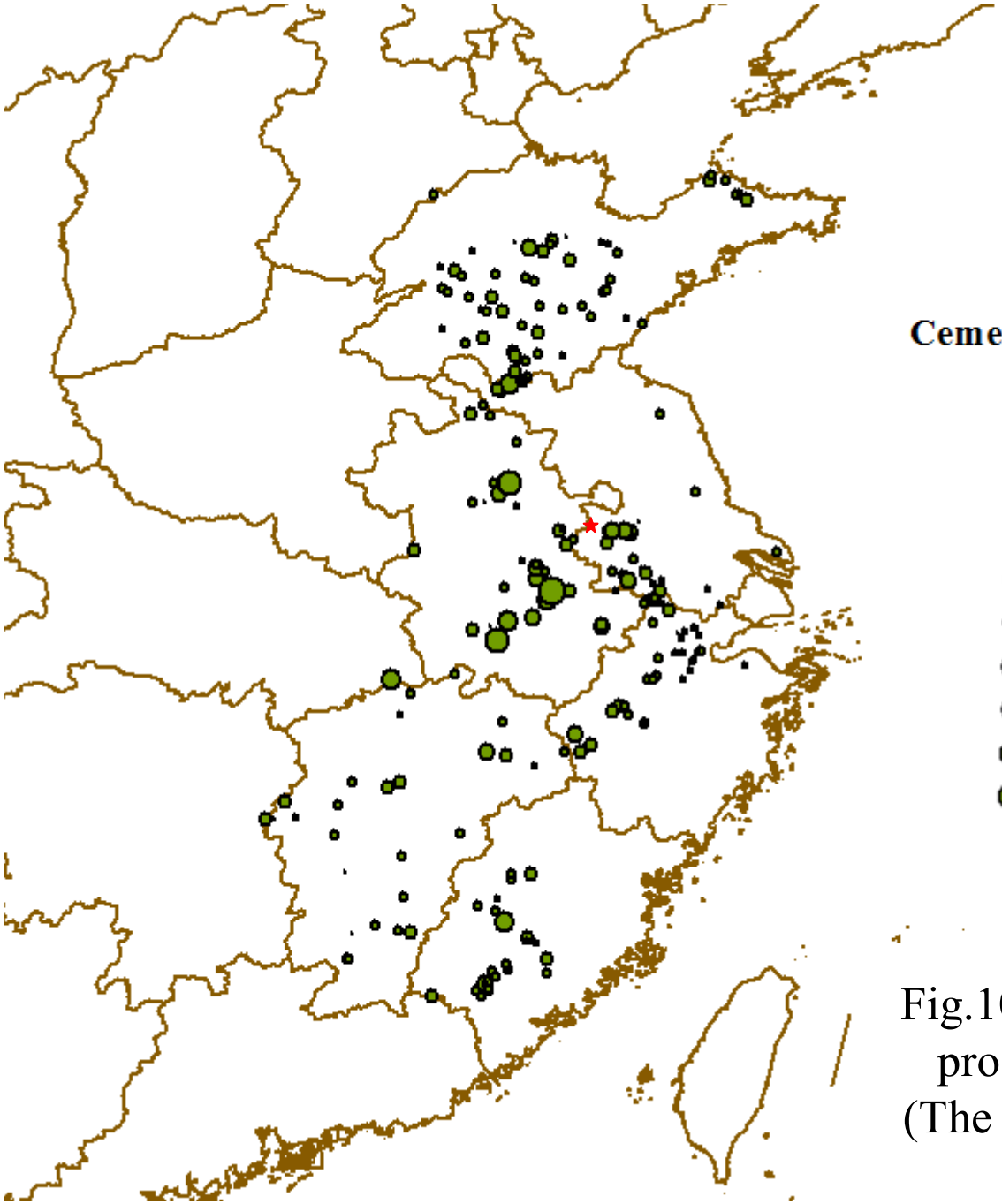

Fig.10 The cement plants and its production in Eastern China. (The red star represents NUIST)

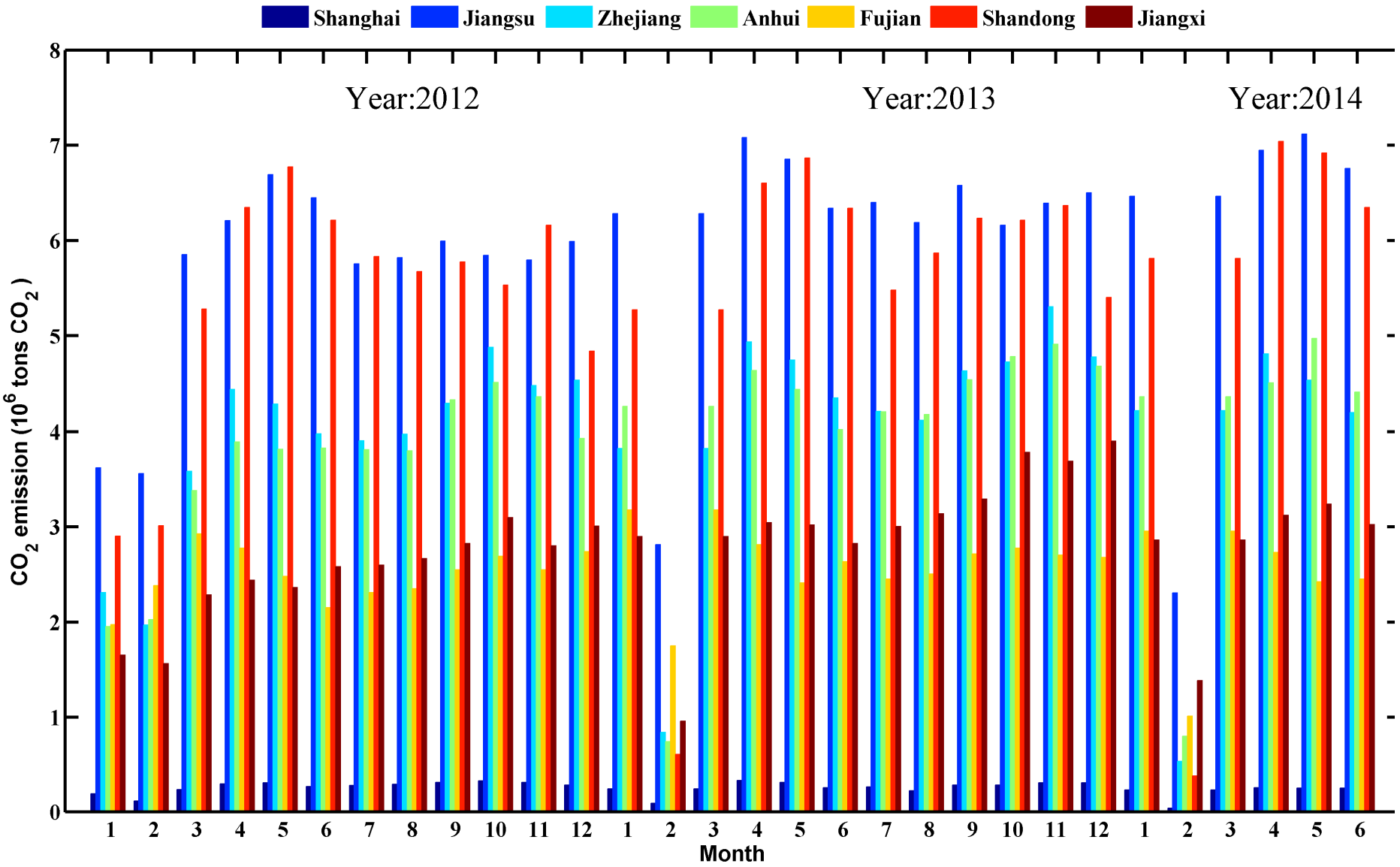

Fig. 11. The CO_2 emission contributed by clink production.

F_C in YRD: 9.75% of F_F (CO_2 mg·m^{-2}·s^{-1}), in this study.

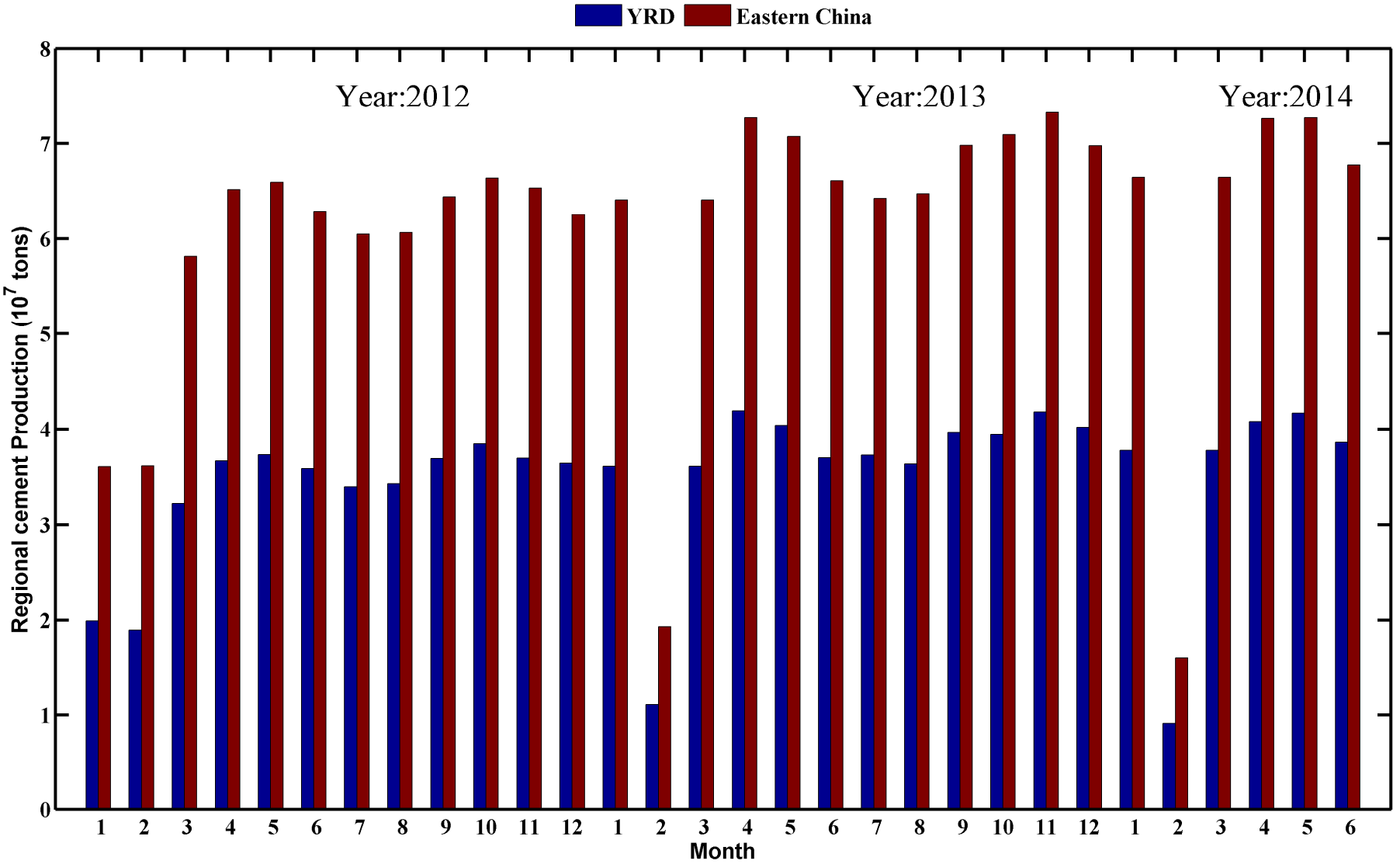

Fig.12. The CO_2 emission contributed by clink production in regional areas.

4.4. Source footprint

- Dataset:

1. Meteorology data: NCEP GDAS 1° ×1° data
2. CO_2 concentration data:

   Picarro G2201-i: From 14th Oct ,2012 to 26th Feb,2013.

   Picarro G1101-i: From 26th Feb ,2013 to 7th July,2014.

- Method (Sigler, 2006):

1. Three 48-hour backward trajectories were simulated per day at 10:00, 13:00 and 16:00 LST.
2. The simulation of height is 1000m.The reasons why I determined 1000m are shown in the next slide.
3. The criterion value were determined from the 85th percentile concentration of all Picarro data for every season.
4. WPSCF was used in this analysis.

Observational Research on Planetary Boundary Layer by Lidar Over Nanjing City

JIANG Jie[1,2], ZHENG Youfei[1,2*], LIU Jianjun[1,3], FAN Jinjin[1,2]

(1.School of Atmospheric Physics, Nanjing University of Information Science and Technology;
2.Jiangsu Key Laboratory of Meteorological Disaster, Nanjing 210044, China;
3.Earth System Science Interdisciplinary Center, University of Maryland, Maryland 20742, USA)

Abstract: In order to study the structural feature of the planetary boundary layer (PBL) over Nanjing City, the height of PBL was inverted by using wavelet covariance method, based on one year's measurements of atmospheric scattering properties by a Mie-scatter Lidar from Nov. 2010 to Oct. 2011. The characteristics of diurnal cycle and seasonal variations of the height of PBL were analyzed and then the influence induced by meteorological conditions was discussed. Results showed that the typical diurnal cycles were found in Nanjing area with low values less than 0.5 km at night and high values greater than lkm at daytime respectively; the maximum mixing layer height has a highest value 1.77 km in spring and a lowest value 1.34 km in winter. A significantly positive relationship between the height of PBL development (maximum mixing layer height) and the surface temperature was found, while a significantly negative relationship with the surface relative humidity was obtained. Clouds can reduce the maximum mixing layer height effectively and reduce the time to get to the maximum mixing layer height.

Key words: lidar; planetary boundary layer; entrainment layer; wavelet covariance

表 2 有云层存在时最大混合层高度和出现时间以及与之对应的月平均值

Table 2 The maximum value of the height of PBL and the moment when the maximum value appears on cloud day and corresponding month mean value

日期	最大混合层高度/km	出现时间	月平均最大混合层高度/km	月平均出现时间
01.17	1.12	14:20	1.28	15:00
03.18	1.71	14:00	1.80	15:14
03.30	1.42	14:40	1.80	15:14
04.14	1.62	15:15	1.75	15:33
04.16	1.65	14:50	1.75	15:33
05.25	1.60	15:20	1.76	15:25
06.23	1.00	13:25	1.35	13:40
07.03	1.20	13:00	1.37	13:25
09.04	1.41	14:05	1.48	14:17
09.18	1.32	14:20	1.48	14:17
09.25	1.5	14:10	1.48	14:17
10.10	1.1	13:15	1.50	14:43
10.16	1.2	14:10	1.50	14:43

- According to Pro Zheng YouFei(郑有飞)'s research, they found the monthly maximum value of the height of PBL during Winter,2010 to Fall,2011 were higher than 1km. The moment when the maximum value occurred also corresponded to my simulation. The results showed the seasonal variation of the height of PBL was Winter<Autumn<Spring<Summer.
- Pro Jiang WeiMei(蒋维楣) found the height of PBL was about 500m in 2002 in Nanjing, which was adopted by Yang Dong (杨栋)'s paper, but Jiang Run(姜润) found the height of PBL in Nanjing was higher than 1km at noon in winter in her Master's graduation paper. What's more, Qi DeLi(齐德利) helped me calculate the height of PBL by running WRF. The results testified that the height of PBL during 2013 to 2014 was about 1km from 10:00-17:00 LST in every months.
- The increasing roughness of land surface due to urbanization (and heat island) might be the main reasons why the height of PBL lifted rapidly in this decade.

Table.10 The seasonal 85th percentile CO_2 concentration.

Season	CO_2 Concentration (ppm)
Autumn,2012	452.87
Winter,2012-2013	456.87
Spring,2013	459.23
Summer,2013	448.17
Autumn,2013	458.73
Winter,2013-2014	467.42
Spring,2014	466.75
Summer,2014	470.90*

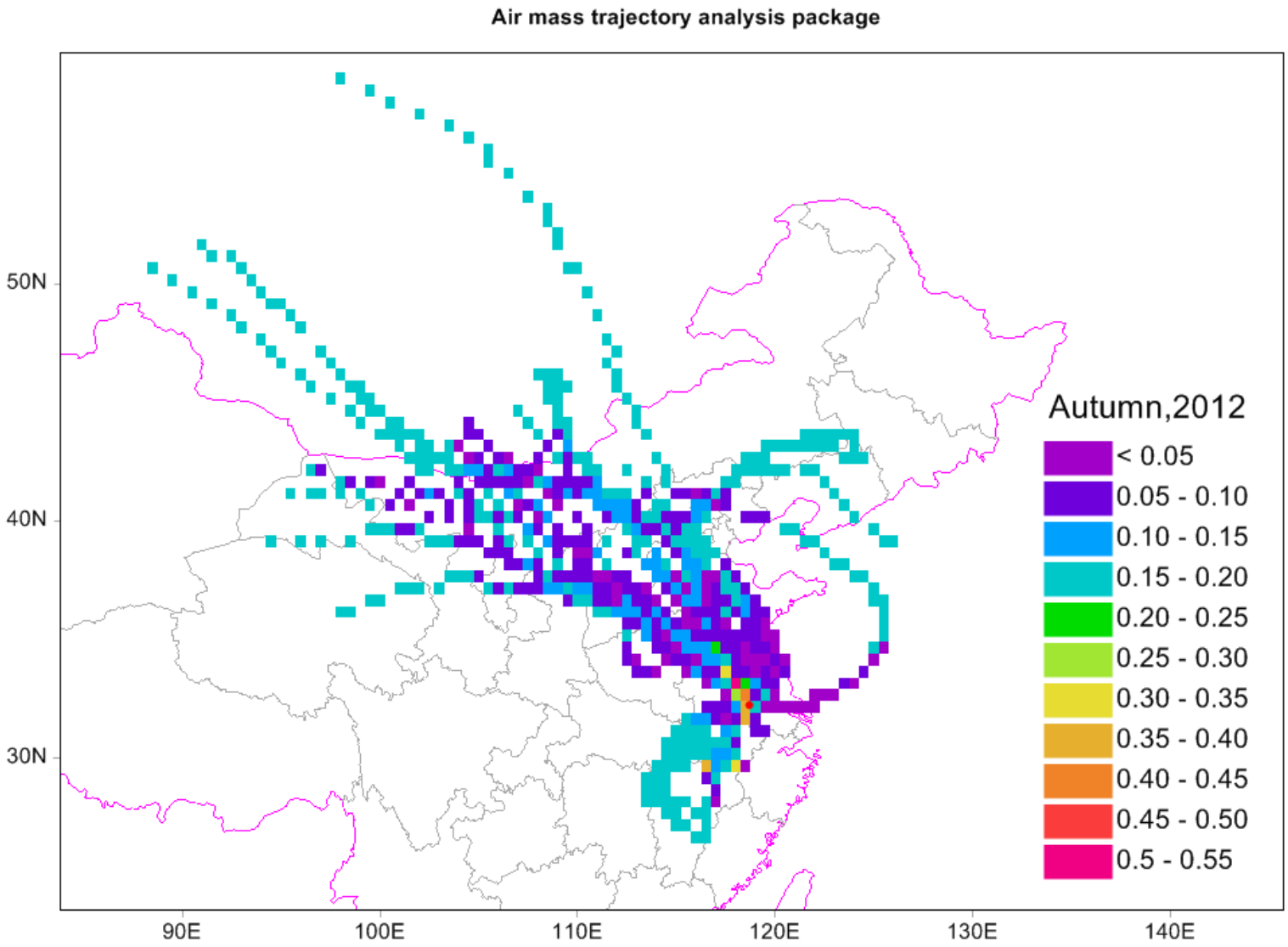

Fig.13 WPSCF probability values during Autumn,2012. (The red circle is the location of Meteorology Building, NUIST,Nanjing.)

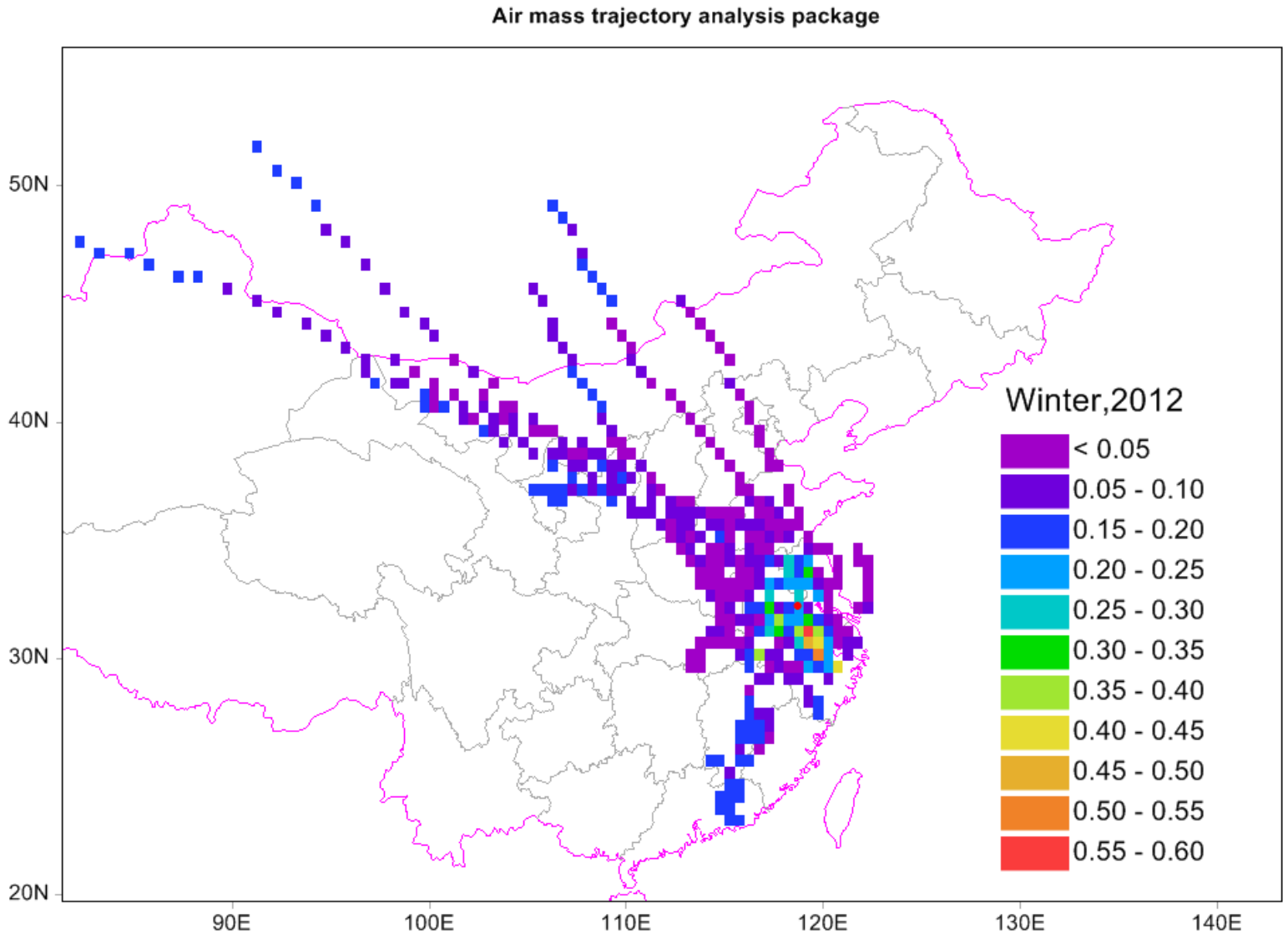

Fig.14 WPSCF probability values during Winter, 2012-2013.

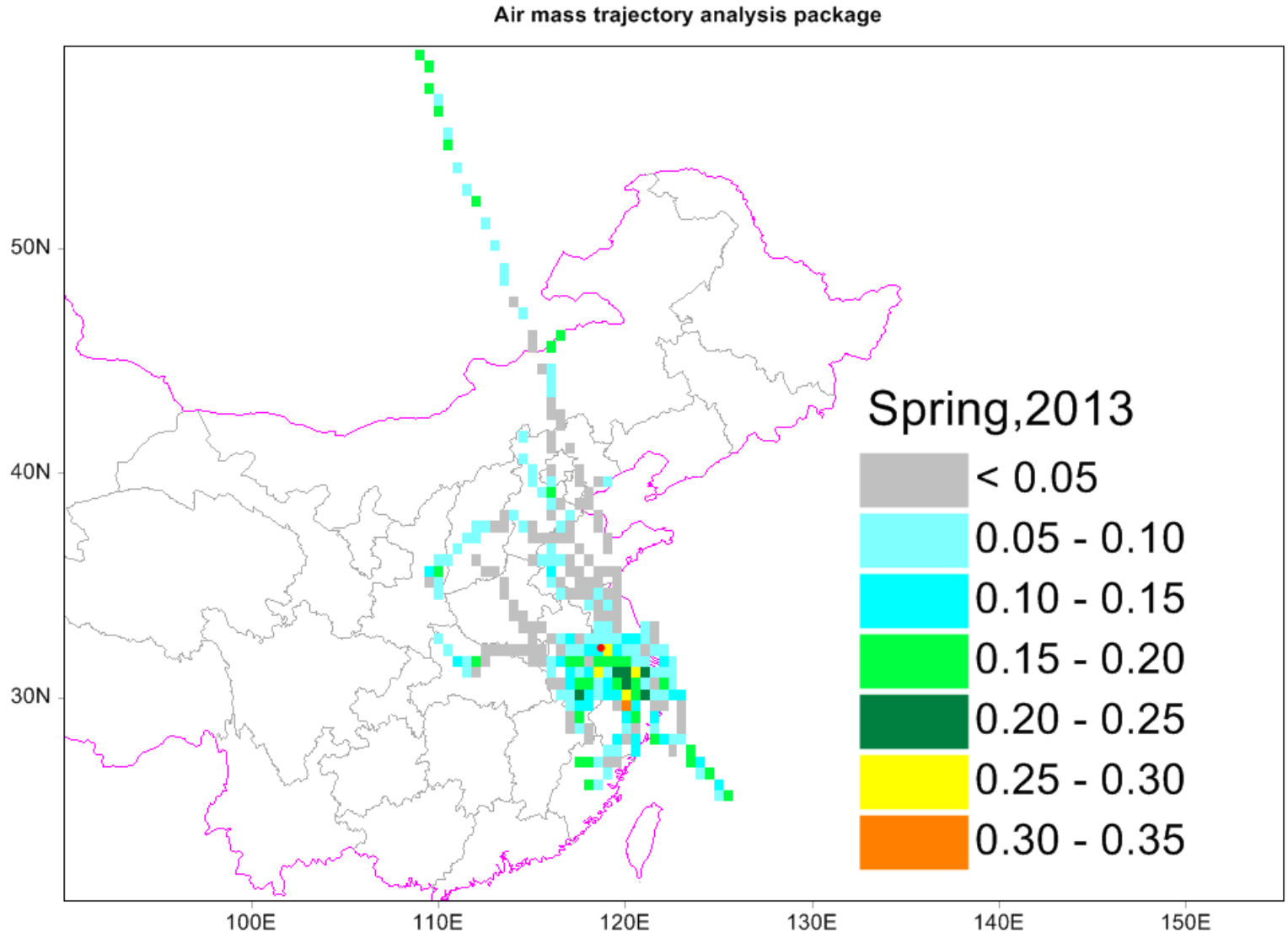

Fig.15 WPSCF probability values during Spring, 2013.

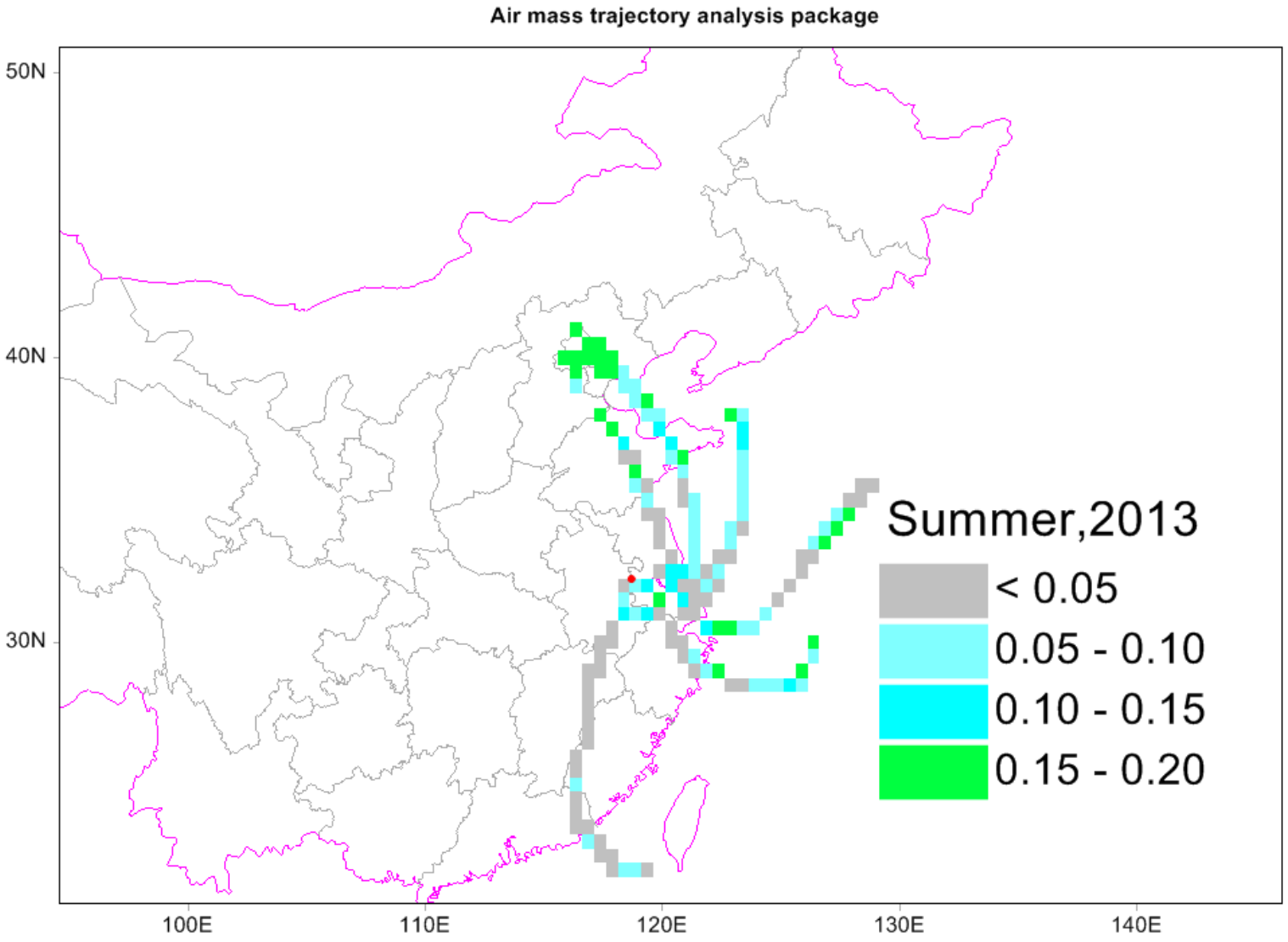

Fig.16 WPSCF probability values during Summer, 2013.

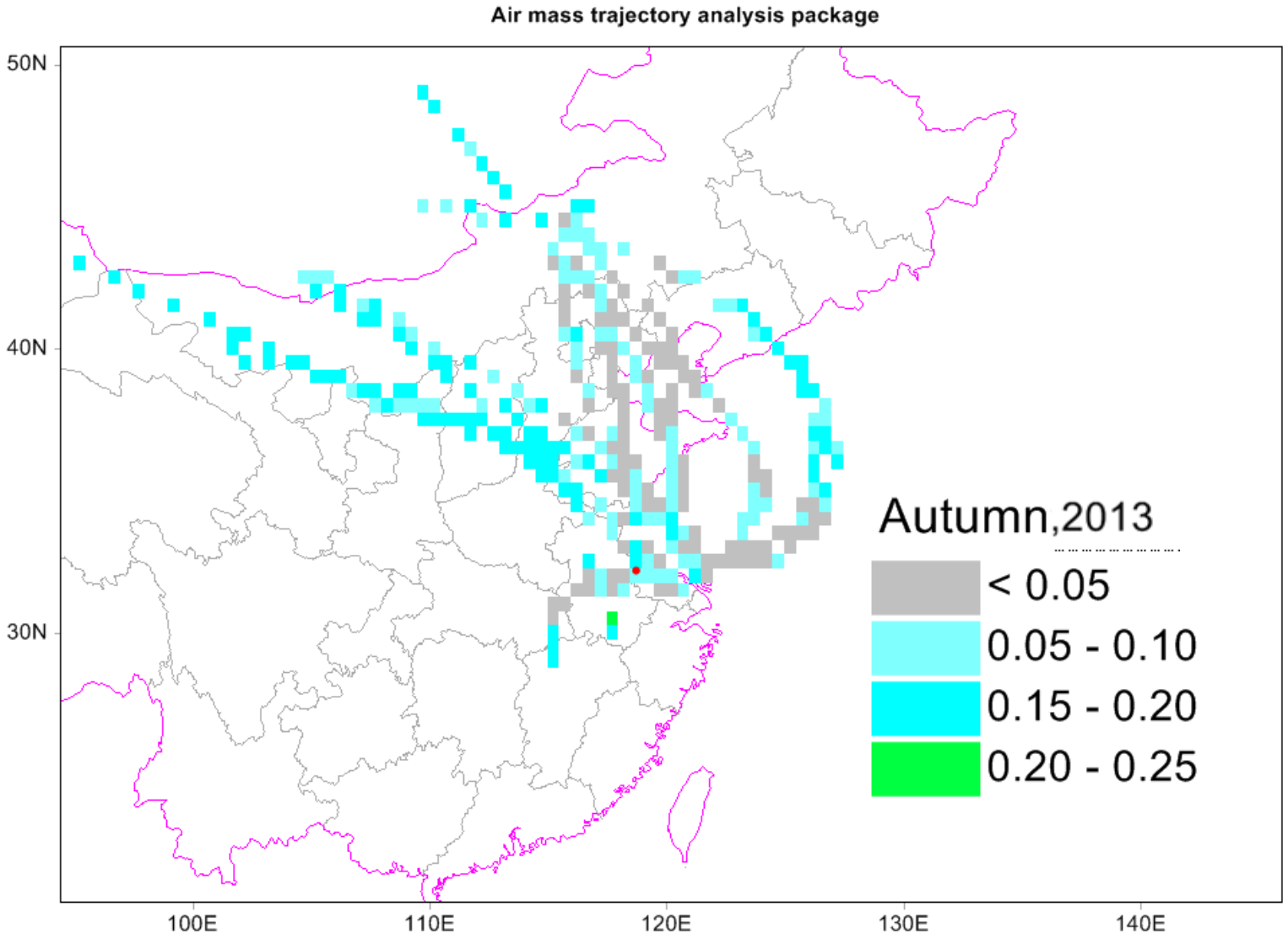

Fig.17 WPSCF probability values during Autumn, 2013.

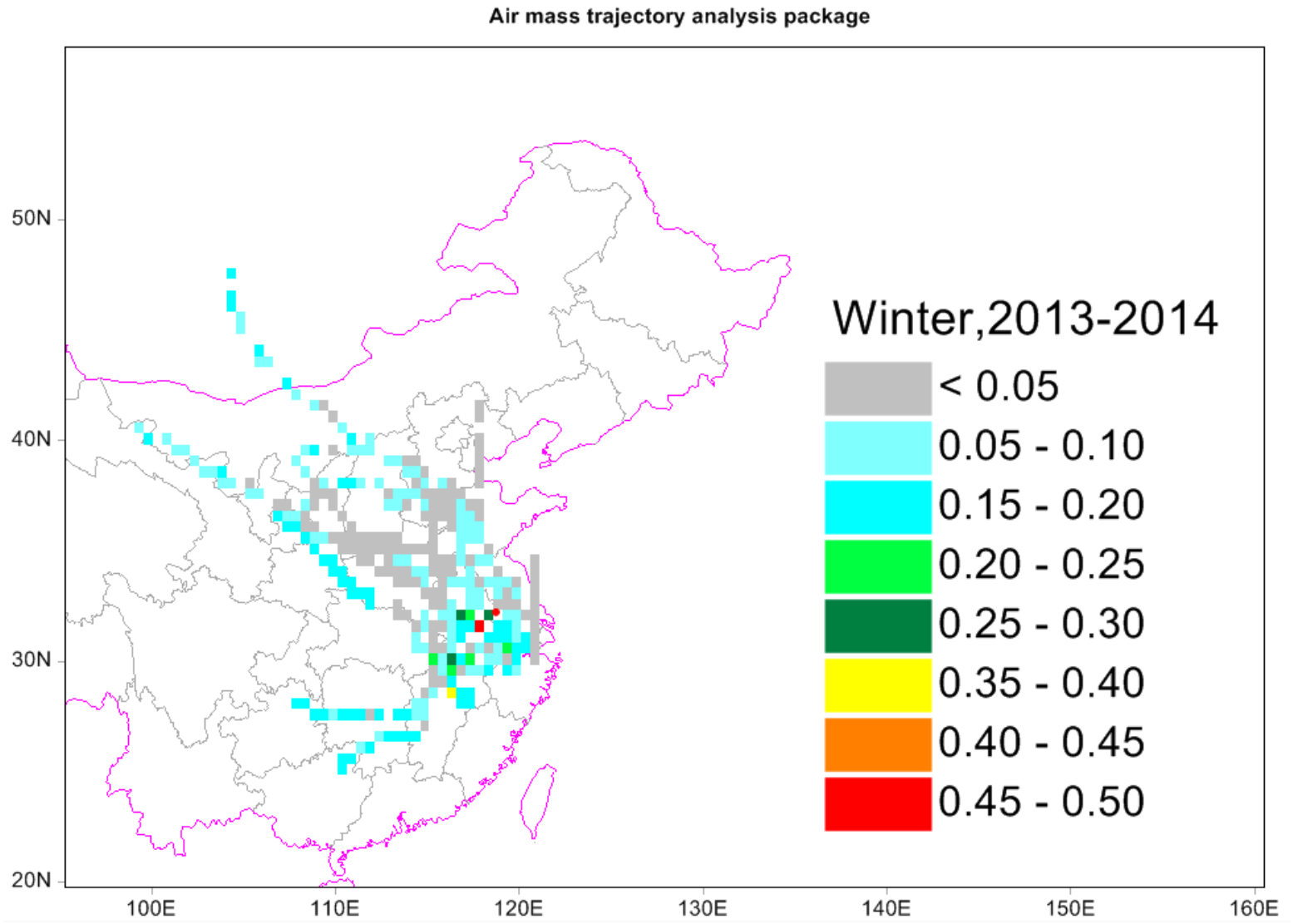

Fig.18 WPSCF probability values during Winter, 2013-2014.

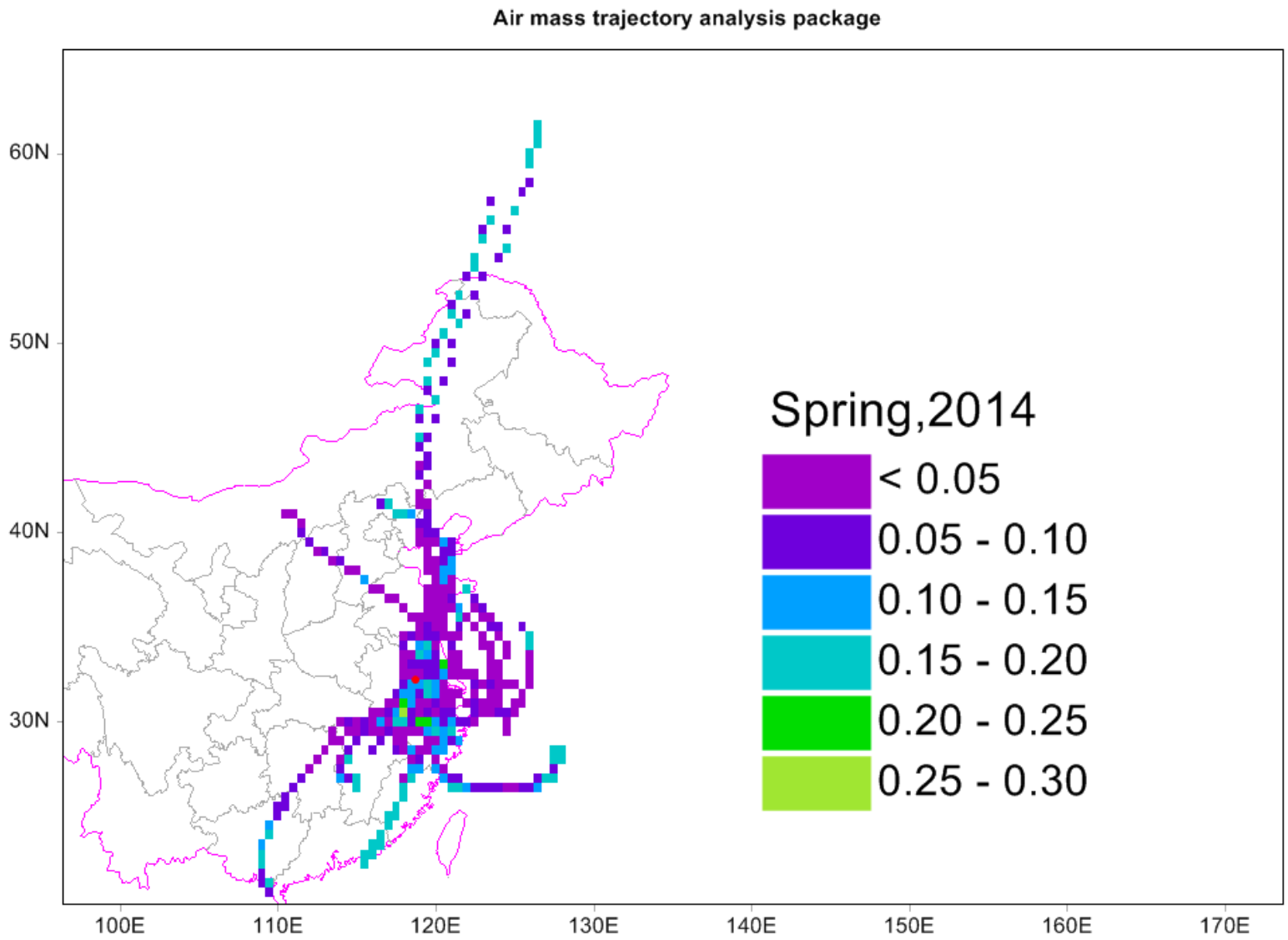

Fig.19 WPSCF probability values in during Spring, 2014.

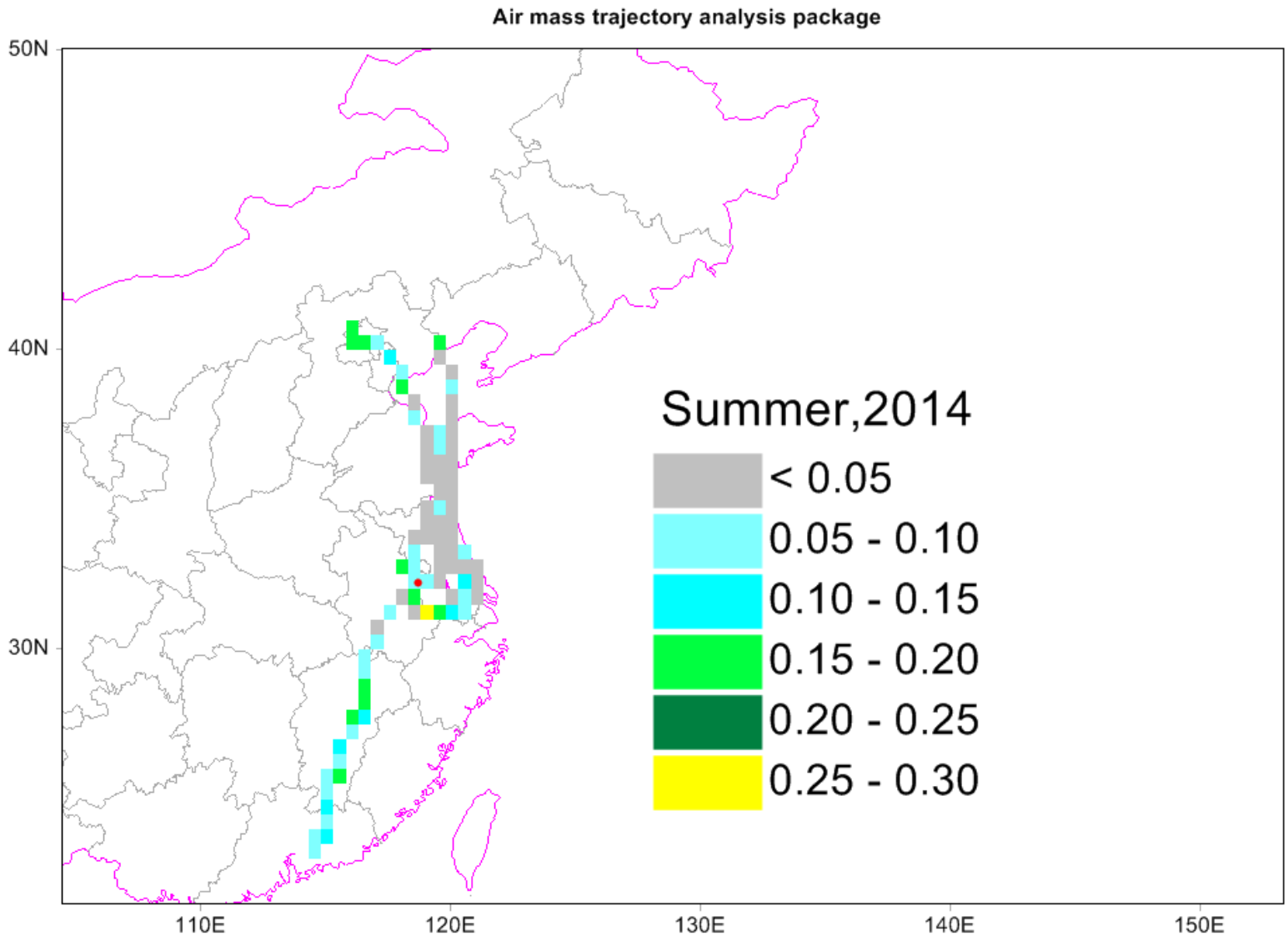

Fig.20 WPSCF probability values in during summer, 2013.

- The source region was strongly influenced by the dominating synoptic systems in four seasons. So the 48-hour back trajectory could reach Russia in winter and Hainan or Taiwan province in summer.
- From autumn,2012 to summer, 2014, the main potential source regions lied in the south of Jiangsu province, the north of Zhejiang province and the east of Anhui province where so many cement plants located in.
- During summer (Fig16 and 20), the potential source region was local areas.
- During winter,2013-2014, the potential source region was Anhui province, which could reach 0.5. But the production in winter was low because of spring festival vacation.

4.5. CO_2 flux in YRD

Table.11. Other CO_2 sources' $\delta^{13}C$.

Carbon Sources	$\delta^{13}C$ (‰)	Reference
Cement	0	Andes,2000
Plant	-26.2	Pataki,2003

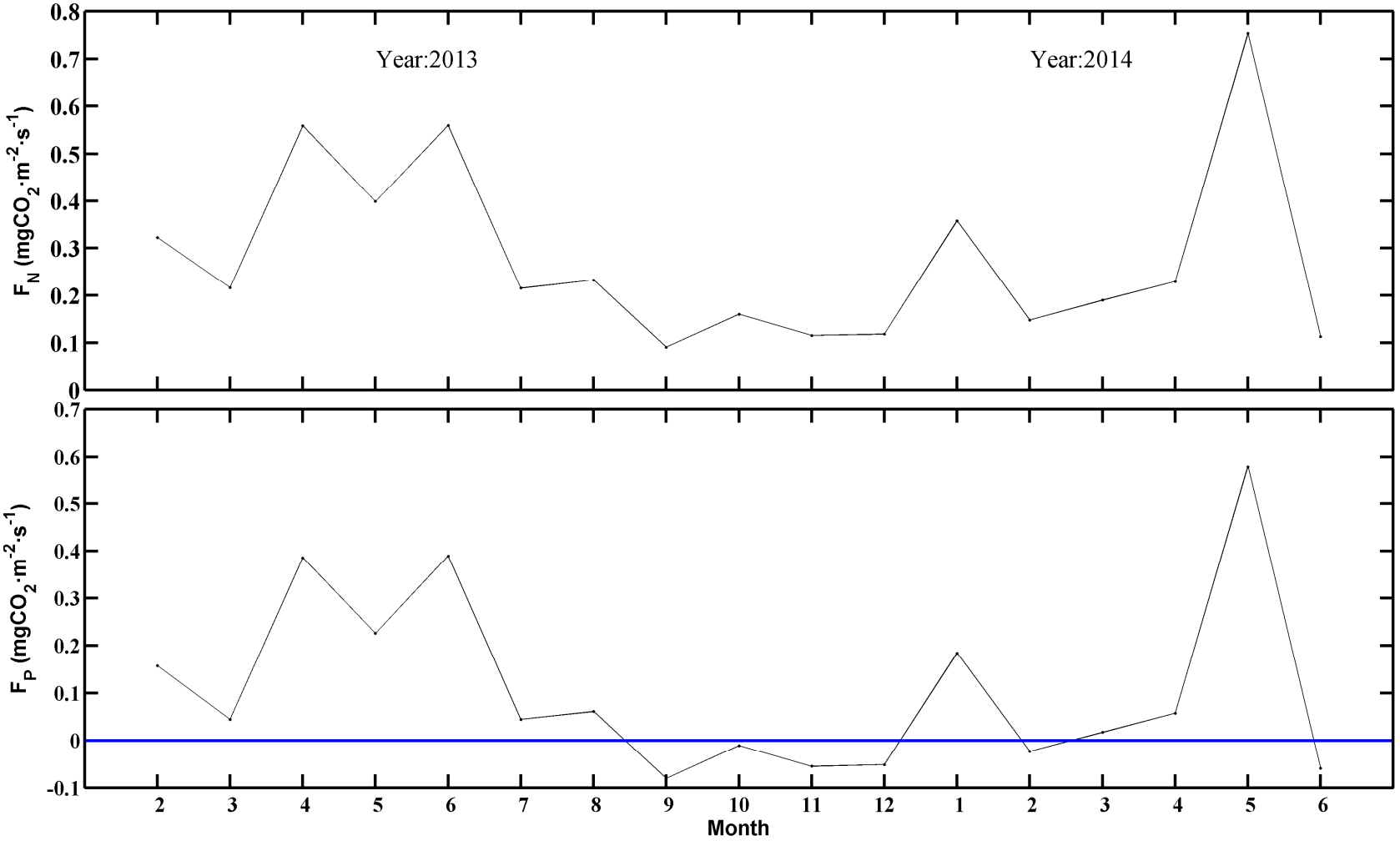

Fig.21. The time series of net CO_2 flux (F_N) and plant CO_2 flux (F_P) in Nanjing.

F_F:57.45%,F_P:38.76%,F_C:3.87% (Feb,2013-Jan,2014)

F_F:58.46%,F_P:39.12%,F_C:3.92% (Feb,2013-Jun,2014)

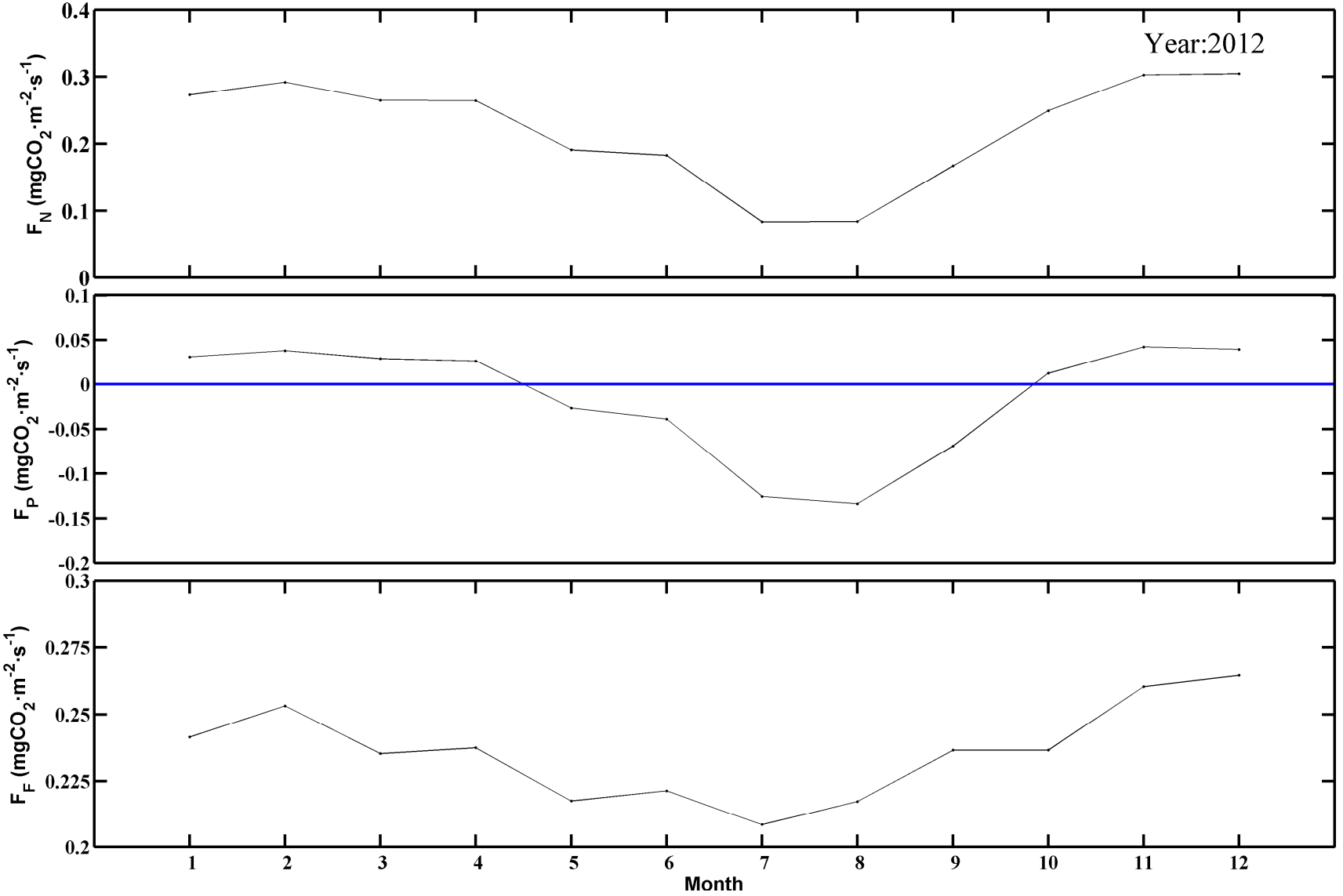

Fig.22. The time series of net CO_2 flux (F_N) and plant CO_2 flux (F_P) according NOAA's carbon tracer (CT) data in 2012 (The magnitude of CO_2 Flux contributed by fire was 10^{-4} ($CO_2 mg \cdot m^{-2} \cdot s^{-1}$)).

Table.13. CO_2 flux in YRD.

Flux (CO_2 $mg \cdot m^{-2} \cdot s^{-1}$)	Net	Plant	Fossil fuel	Clink	Fire
Picarro	3.347	1.297	1.922	0.128	
CT	2.658	-0.175	2.830		0.003

5. Conclusion

- 1. $\delta^{13}C_S$ calculated by Miller-Tans method was less negative than Keeling plot. Miller-Tan method had a better performance to calculate $\delta^{13}C_S$. $\delta^{13}C$ was highest in summer while lowest in spring. The D-value could reach about 1‰ .

- 2. The mixing ratio $\delta^{13}C$ of fossil combustion was -25.59‰ with a high uncertainty.

- 3. The source region was strongly influenced by dominating synoptic systems in four seasons.

- 4. Fossil fuel combustion could contribute 0.1744 CO_2 $mg \cdot m^{-2} \cdot s^{-1}$ while cement production could emit 0.0670 CO_2 $mg \cdot m^{-2} \cdot s^{-1}$ in YRD in 2012 .

- 5. The magnitude of net CO_2 flux and plant CO_2 flux calculated by using ^{13}C isotope was right, but it still need be adjusted to adopt the seasonal trend and former research.

6. Next work

- 1. Take more industrial potential CO_2 contributors into consideration, such as synthesis ammonia, pig iron and crude steel.

- 2. To decrease the uncertainty of $\delta^{13}C_S$ by removing more outliners.

- 3. To complete analyzing the sensitivity and uncertainty of mean contributions by each fractional CO_2 flux in YRD.

- 4. Try to focus on the influence of environmental regulations caused by Youth Olympic Games this summer in Nanjing on regional atmospheric CO_2 and its stable isotope ratio.

Thank You!